Oral Presentation

The 7th TSME International Conference on Mechanical Engineering
13-16 December 2016

TSME ICOME 2016
Mechanical Engineering Innovation for Green Society

AMM0015

A Study on Tolerances Design of Parallel Link Robots Based on Mathematical Models

Ryo Takematsu[1,*], Wiroj Thasana[2], Koji Iwamura[3], Yoshitaka Tanimizu[1]and Nobuhiro Sugimura[3]

[1] Mechanical Engineering, Graduate School of Engineering, Osaka Prefecture University
1–1 Gakuen-cho, Naka-ku, Sakai-shi, Osaka 599–8531, Japan
[2] Advanced Design and Manufacturing Technology Research Laboratory, Thai-Nichi Institute of Technology
1771/1 Pattanakarn Rd., Suanluang, Bangkok 10250, Thailand
[3] Graduate School of Humanities and Sustainable System Science, Osaka Prefecture University
1–1 Gakuen-cho, Naka-ku, Sakai-shi, Osaka 599–8531, Japan
[*] Corresponding Author: sv101036@edu.osakafu-u.ac.jp, Tel. +81722549211

Abstract

The precision and accuracy of the movement of the parallel link robots are one of the key features that are essential in the production processes, which control the position and speed of the mechanism linking, and have the movement of the final control motors mounted within the linkage mechanism on the basis of a number of mathematical models. Recently, 3-dimensional CAD/CAE systems are widely applied and mechanical design has become complicated. Therefore, the tolerance design of the products is becoming more difficult and complicated. The objective of this research is to propose a mathematical model of the parallel link robots, which applies to tolerance designs for the parallel link robots based on the geometric tolerances of the components. The proposed method provides us with a systematic method to design the geometric dimensioning and tolerancing of the components, under the constraints of the kinematic motion accuracy.

Keywords: Tolerance Design, Geometric Dimensioning and Tolerancing, Modeling, Kinematic Motion Deviations.

1. Introduction

The precision and accuracy of the movement of the parallel link robots are one of the key features that are essential in the production processes, which control the position and speed of the mechanism linking, and have the movement of the final control motors mounted within the linkage mechanism on the basis of a number of mathematical models. Recently, 3-dimensional CAD/CAE systems are widely applied and mechanical design has become complicated. Therefore, the period of the tolerance designs of the mechanical products has become shortened and more difficult. In the designing phase, it is required that tolerances of the components with high accuracy are set properly. In the production process, it is required to keep the geometric and dimensional deviations within the range of tolerances.

As regards the geometric tolerances, some researches have been carried out to deal with the dimensional tolerances and the geometric tolerances, aimed at realizing statistical analysis and design methodologies for 3-dimensional machine products [1-11]. In the previous papers, a systematic procedure determines the tolerance values of the guide-ways theoretically under the constraints on the basis of kinematic motion deviations of 5-axis machining centers by applying mathematical models.

The objective of the present research is to propose a mathematical model to deal with parallel link robots which are applied to assembly works and picking works for utilizing high-speed. The mathematical models are proposed to represent the kinematic motion deviations of parallel link robots, on the basis of the dimensions and geometric tolerances of the components, and are applied to systematic procedure which determine the both dimensional tolerances and geometric tolerances of the guide-ways under the constraints on the basis of kinematic motion deviations of parallel link robots.

2. Geometric Tolerances and Deviations of Features [7-9]

The geometric tolerances of the features specify the allowable areas named “tolerance zones,” which constrain the position and orientation deviations of the associated features against the nominal features, as shown in Fig. 1 (a). The associated features and the nominal features mean the features of the manufactured products and the ideal features defined in the design phase, respectively. The geometric deviations of the associated features from the nominal features are represented by sets of parameters named “deviation parameters.” For example, one position parameter w and two rotational parameters α and β are required to represent the geometric deviations of the associated plane features against the nominal plane features, for the case where the tolerance zone is given by the area between a pair of parallel planes. In the research, the followings are assumed for the ease of the modeling and the analysis of the geometric deviations.

(1) The deviation parameters δ_i representing the position and orientation deviations of the associated features follow the normal distribution $N(\mu_i, \sigma_i)$, and μ_i =0. Where, μ_i and σ_i are the

mean values and the standard deviations, respectively.

(2) The manufacturing processes of the components are well controlled, and the proportion of the non-conforming components, which means the toleranced features exceed the tolerance zones, is as small as a value P_d called "Defective rate".

(3) Eq. (1) represents the relationships between the standard deviations σ_i of the deviation parameters of the tolerance features and the maximum values of the deviation parameters.

$$\sigma_i = \delta_{imax}/C_{Pd} \tag{1}$$

Where,

δ_{imax} : Maximum values of the deviation parameters δ_i, if the other deviation parameters are $\delta_j = 0$, $(i \neq j)$.

C_{P_d} : A constant representing the ratio of the maximum values δ_{imax} and the standard deviations σ_i.

Let us consider a case of the plane feature shown in Fig. 1(a), as an example. The maximum values δ_{imax} are given as follows.

$$\delta_1 = w, \delta_2 = \alpha, \delta_3 = \beta$$

$$\delta_{1max} = \frac{t}{2}, \delta_{2max} = \frac{t}{L_1}, \delta_{3max} = \frac{t}{L_2} \tag{2}$$

Where,

L_1, L_2 : Length and width of the plane feature.

t : Tolerance values, e.g. the distance between two planes representing the tolerance zones.

From Eqs. (1) - (2), the standard deviation of three parameters are given as follows.

$$\sigma_1 = \frac{t}{2C_{Pd}}, \sigma_2 = \frac{t}{L_1 C_{Pd}}, \sigma_3 = \frac{t}{LC_{Pd}} \tag{3}$$

The following equation gives the conditions that the plane features are included within the tolerance zone between a pair of planes.

$$-\frac{t}{2} \leq \delta_1 + \frac{L_1\delta_2}{2} + \frac{L_2\delta_3}{2} \leq \frac{t}{2} \tag{4}$$

The probability that the tolerance features are included the tolerance zone is given by the following equation. This probability $1 - P_d$ means yield rate.

$$1 - P_d = \left(\frac{2}{\sqrt{2\pi}}\right)^3 \int_0^{C_{Pd}} \int_0^{C_{Pd}-x_1} \int_0^{C_{Pd}-x_1-x_2} \left(\prod_{i=1}^{3} \exp\left(-\frac{x_i^2}{2}\right)\right) dx_3 dx_2 dx_1 \tag{5}$$

Where,

$$x_1 = \frac{2C_{P_d}\delta_1}{t}, x_2 = \frac{L_1 C_{P_d}\delta_2}{t}, x_3 = \frac{L_2 C_{P_d}\delta_3}{t}$$

If the defective rate P_d is set to 0.27%, the constant C_{Pd} can be estimated as "C_{Pd} = 5.83", through the numerical analysis of Eq. (5).

In the case of a cylinder shown in Fig. 1(b), the following equation gives the standard deviations of the parameters.

$$\begin{aligned} &\delta_1 = u\ \delta_2 = w, \delta_3 = \alpha, \delta_4 = \gamma \\ &\delta_{1max}, \delta_{2max} = \frac{t}{2}, \delta_{3max}, \delta_{4max} = \frac{t}{L} \\ &\sigma_1, \sigma_2 = \frac{t}{2C_{Pd}}, \sigma_3, \sigma_4 = \frac{t}{LC_{Pd}} \end{aligned} \tag{6}$$

In this case, the C_{P_d} is estimated as "C_{P_d}= 5.06", of the defective rate P_d is set to be 0.27%.

In the case of a sphere shown in Fig.1(c), the following equation gives the standard deviations of the parameters.

$$\begin{aligned} &\delta_1 = u\ \delta_2 = v, \delta_3 = w \\ &\delta_{1max}, \delta_{2max}, \delta_{3max} = \frac{t}{2}, \sigma_1, \sigma_2, \sigma_3 = \frac{t}{2C_{Pd}} \end{aligned} \tag{7}$$

In this case, the C_{P_d} is estimated as "C_{P_d}=3.57", of the defective rate P_d is set to be 0.27%.

The C_{P_d} varies with features because it is calculated by Eq.(5) and the number of parameter varies with features.

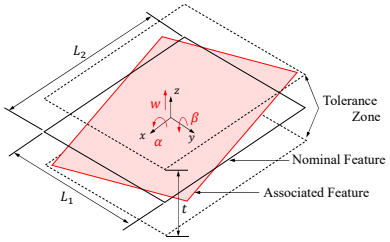

(a) Plane feature

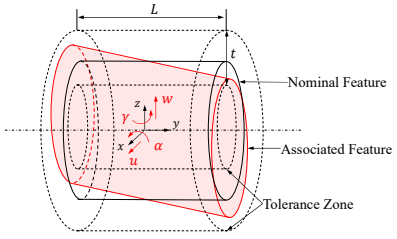

(b) Cylinder feature

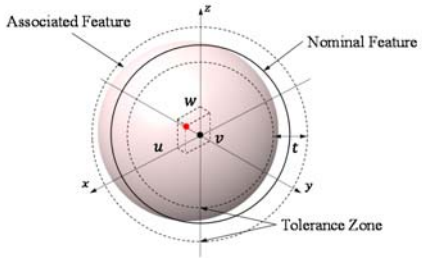

(c) Sphere Feature

Fig. 1 Definition of geometric tolerance of features

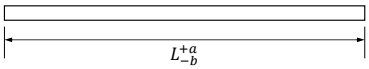

Fig. 2 Tolerance zone of the link errors

The dimensional tolerances are shown in Fig.2, the tolerance zone values are expressed as $t = a + b$, assumed to be $\pm 3\sigma$ and the following equation gives the standard deviation of the parameters. In this case, the C_{P_d} is estimated as "C_{P_d}= 3", of the defective rate P_d is set to be 0.27%.

$$\delta_{max} = \frac{t}{2}, \sigma = \frac{t}{2C_{P_d}} \quad (8)$$

3. Kinematic Analysis of Parallel Link Robots

3.1 System description

The parallel link robot in this study is shown in Fig. 3. It has three degrees of freedom (DOF) and motion along X, Y, Z-axis that consist a fixed base, three branched chains and the active links. These are connected to the servo motors, and one end of each passive link is connected to its active link by spherical joints. While the opposite end side is connected to the moving end-effector. A schematic diagram of the 3-DOF parallel link robot and its parameters are shown in Fig.4,5.

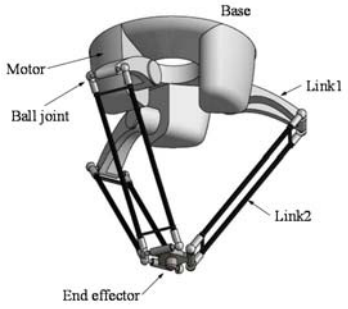

Fig. 3 The parallel link robot

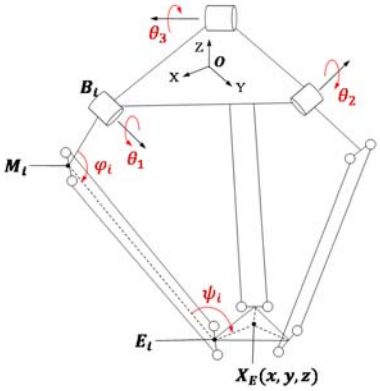

Fig. 4 The kinematic diagram

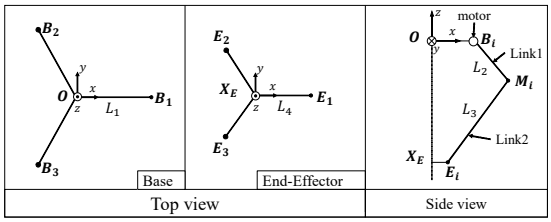

Fig. 5 The kinematic parameters

3.2 Inverse kinematics analysis

Denavit Hartenberg has proposed the D-H method, which is commonly utilized in robot kinematic models. In this research, inverse kinematics analysis is considered to determine the active link position angle $\theta_i (i=1,2,3)$ according to the position (x, y, z) of the moving end-effector. As three chains have the same structure and form of motions, we can consider them together.

The kinematic diagram is shown in Fig. 4, the state of three applicable constraints that the lower lengths must have to accuracy, constant length L_3 is shown in Eq. (9).

$$L_3 = |\boldsymbol{E_i} - \boldsymbol{M_i}| \quad (i = 1,2,3) \quad (9)$$

In order to convenient square both side of the constraint equations in Eq. (9) to avoid the square-root, the constraint equation is given in Eq. (10).

$$L_3^2 = |\boldsymbol{E_i} - \boldsymbol{M_i}|^2 \quad (i = 1,2,3) \quad (10)$$

The variable values are the position $\boldsymbol{X}_E = \{x, y, z\}^T$ of the end-effector. The constant vector values are points $\boldsymbol{B_i}, \boldsymbol{E_i}$ were given previously. The vectors $\boldsymbol{M_i}$ are dependent on the joint variables $\boldsymbol{\theta} = \{\theta_1, \theta_2, \theta_3\}^T$ by applying the following equation.

$$\boldsymbol{M_1} = \begin{Bmatrix} L_1 + L_2 \cos\theta_1 \\ 0 \\ -L_2 \sin\theta_1 \end{Bmatrix}$$
$$\boldsymbol{M_2} = \begin{Bmatrix} \frac{1}{2}L_1 - \frac{1}{2}L_2 \cos\theta_2, \\ \frac{\sqrt{3}}{2}L_1 + \frac{\sqrt{3}}{2}L_2 \cos\theta_2 \\ -L_2 \sin\theta_2 \end{Bmatrix} \quad (11)$$
$$\boldsymbol{M_3} = \begin{Bmatrix} \frac{1}{2}L_1 - \frac{1}{2}L_2 \cos\theta_3, \\ \frac{\sqrt{3}}{2}L_1 - \frac{\sqrt{3}}{2}L_2 \cos\theta_3 \\ -L_2 \sin\theta_3 \end{Bmatrix}$$

$$\boldsymbol{E_1} = \{x + L_4, y, z\}$$
$$\boldsymbol{E_2} = \left\{x - \frac{L_4}{2}, y + \frac{\sqrt{3}}{2}L_4, z\right\} \quad (12)$$
$$\boldsymbol{E_3} = \left\{x - \frac{L_4}{2}, y - \frac{\sqrt{3}}{2}L_4, z\right\}$$

From Eqs. (9) - (12), the three independent equations are obtained in the Eq. (13), as shown below.

$$A_i \cos\theta_i + B_i \sin\theta_i = C_i \quad (13)$$

where:

$$A_1 = x + L_4 - L_1, B_1 = z, C_1 = \frac{L_3^2 - L_2^2 - A_1^2 - y^2 - z^2}{2L_2}$$

$$A_2 = \frac{1}{2}\left(D_2 + \sqrt{3}E_2\right), B_2 = z, C_2 = \frac{L_3^2 - L_2^2 - D_2^2 - E_2^2 - z^2}{2L_2}$$

$$D_2 = x - \frac{1}{2}L_4 + \frac{1}{2}L_1, \quad E_2 = y + \frac{\sqrt{3}}{2}L_4 - \frac{\sqrt{3}}{2}L_1$$

$$A_3 = \frac{1}{2}\left(D_3 + \sqrt{3}E_3\right), B_3 = z, C_3 = \frac{L_3^2 - L_2^2 - D_3^2 - E_3^2 - z^2}{2L_2}$$

$$D_3 = x - \frac{1}{2}L_4 + \frac{1}{2}L_1, \quad E_3 = y + \frac{\sqrt{3}}{2}L_4 + \frac{\sqrt{3}}{2}L_1$$

According to the assembly mode, inverse kinematics analysis gives θ_i as Eq. (14).

$$\theta_i = -\tan^{-1}(B_i, A_i) - \tan^{-1}\left(C_i, \sqrt{A_i^2 + B_i^2 - C_i^2}\right) \quad (14)$$

For the angle between Link 1 and Link 2, Link 2 and end-effector are determined by the inner product of $\boldsymbol{M_iB_i}$, $\boldsymbol{M_iE_i}$, $\boldsymbol{E_iM_i}$ and $\boldsymbol{E_iX_E}$, respectively. The equation is given in Eq. (15).

$$\varphi_i = \cos^{-1}\left(\frac{\boldsymbol{M_iB_i}\cdot\boldsymbol{M_iE_i}}{|\boldsymbol{M_iB_i}||\boldsymbol{M_iE_i}|}\right)$$

$$\psi_i = \cos^{-1}\left(\frac{\boldsymbol{E_iM_i}\cdot\boldsymbol{E_iX_E}}{|\boldsymbol{E_iM_i}||\boldsymbol{E_iX_E}|}\right) \quad (15)$$

4. Modeling of Parallel Link Robots

The model of the parallel link robot is formulated by the kinematic motion matrixes. The matrixes are consistency to relate the kinematic motion deviations among bearings, spherical joints, and links, respectively. It is predicted from geometric deviations of guide-ways and dimensional deviations of the length of links. The method to obtain geometric deviations from geometric dimensioning and tolerancing are explained in the previous section.

4.1 Kinematic motion deviations of motors

The model and kinematic motion matrix of motors are shown in Fig. 6 and Eq. (16). The standard deviations of parameters $\delta\alpha, \delta\gamma, \delta x, \delta y, \delta z$ are calculated by Eqs. (3) - (6), as shown in the following equation.

$$A_5^{\sigma}(\theta) = \begin{pmatrix} \cos\theta & \delta\gamma_{\theta 1} & \sin\theta & \delta x_\theta \\ \delta\gamma_{\theta 2} & 1 & \delta\alpha_{\theta 1} & \delta y_\theta \\ -\sin\theta & \delta\alpha_{\theta 2} & \cos\theta & \delta z_\theta \\ 0 & 0 & 0 & 1 \end{pmatrix} \quad (16)$$

Where,

$\delta\alpha_{\theta 1} = \gamma_{ia}\sin\theta - \alpha_{ia}\cos\theta + \alpha_{jb}$

$\delta\alpha_{\theta 2} = -\gamma_{jb}\sin\theta - \alpha_{jb}\cos\theta + \alpha_{ia}$

$\delta\gamma_{\theta 1} = \gamma_{jb}\cos\theta - \alpha_{jb}\sin\theta - \gamma_{ia}$,

$\delta\gamma_{\theta 2} = \gamma_{ja}\cos\theta + \alpha_{ja}\sin\theta - \gamma_{jb}$

$\delta x_\theta = \frac{1}{2}\left(-2\delta x_{jb} + l_1\gamma_{jb} + l_4\gamma_{jb}\right)\cos\theta - (l_1 + l_4)\gamma_{ia} - \frac{1}{2}\left(2\delta z_{jb} + l_1\alpha_{jb} + l_4\alpha_{jb}\right)\sin\theta + \delta x_{ia}$

$\delta y_\theta = \delta y_{ic} - \delta y_{jc}$

$\delta z_\theta = \frac{1}{2}\left(-2\delta x_{jb} + l_1\gamma_{jb} + l_4\gamma_{jb}\right)\sin\theta + (l_1 + l_4)\alpha_{ia} - \frac{1}{2}\left(2\delta z_{jb} + l_1\alpha_{jb} + l_4\alpha_{jb}\right)\cos\theta + \delta z_{ia}$

α_{mn}, γ_{mn} : Orientation deviations of guide-way n in Unit-m $(m = i, j, n = a, b)$

$\delta x_{mn}, \delta y_{mn}, \delta z_{mn}$: Position deviations of guide-way n in Unit-m $(m = i, j, n = a, b)$

4.2 Kinematic motion deviations of spherical joints

The model and kinematic motion matrix of ball-joints are shown in Fig. 5 and Eq.(17). The standard deviations of parameters $\delta x, \delta y, \delta z$ are calculated by Eq. (7), as shown in the following equation.

$$A_6^{\sigma}(\varphi) = \begin{pmatrix} \cos\varphi & -\sin\varphi & 0 & \delta x_\varphi \\ \sin\varphi & \cos\varphi & 0 & \delta y_\varphi \\ 0 & 0 & 1 & \delta z_\varphi \\ 0 & 0 & 0 & 1 \end{pmatrix} \quad (17)$$

Where,

$\delta x_\varphi = -\delta x_d\cos\varphi + \delta y_d\sin\varphi + \delta x_e$,

$\delta y_\varphi = -\delta x_d\sin\varphi - \delta y_d\cos\varphi + \delta y_e$,

$\delta z_\varphi = \delta z_e - \delta z_d$

$\delta x_n, \delta y_n, \delta z_n$: Position deviations of guide-way n

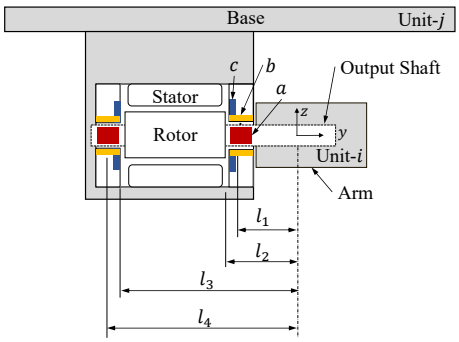

Fig. 6 The model of motors

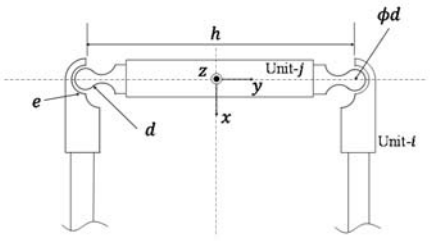

Fig. 7 The model of spherical joints

4.3 Modeling of kinematic motions of parallel link robots

The position $\boldsymbol{X_E}$ of the end-effector is determined by the position E_1, E_2, E_3. E_i are given in the following Eq. (18).

$$\boldsymbol{E_i} = A_1(L_1)A_5^{\sigma}(\theta)A_1(L_2)A_4(\alpha_i) \\ A_6^{\sigma}(\pi-\varphi_i)A_1(L_3)A_4(\beta_i)A_6^{\sigma}(\pi-\psi_i) \quad (18)$$

Where,

$A_1(L_i)$: Translation between the coordinates system

$A^4(\alpha_i, \beta_i)$: Rotation between the coordinates system

$A^5(\theta)$: Rotation of the motors

$A^6(\pi-\varphi_i, \pi-\psi_i)$: Rotation of the spherical joints

Then, the position $\boldsymbol{X_E}$ is calculated by Eq. (19) because $\boldsymbol{X_E}$ is the gravity center of the positions E_1, E_2, E_3.

$$\sigma_{X_E} = (\sigma_x, \sigma_y, \sigma_z)$$

$$\sigma_x = \frac{1}{3}\sqrt{\sigma_{x_1}^2 + \sigma_{x_2}^2 + \sigma_{x_3}^2}, \sigma_y = \frac{1}{3}\sqrt{\sigma_{y_1}^2 + \sigma_{y_2}^2 + \sigma_{y_3}^2}, \quad (19)$$

$$\sigma_z = \frac{1}{3}\sqrt{\sigma_{z_1}^2 + \sigma_{z_2}^2 + \sigma_{z_3}^2}$$

Where,

$\sigma_{xi}, \sigma_{yi}, \sigma_{zi}$: Standard deviation of the position E_i

5. Tolerance Design

The design a suitable set of tolerance values of mechanical products plays an important role from the viewpoint of the both product quality and production costs. The tolerance design is considered here means the allocation processes of the tolerance values. In order to reduce the manufacturing cost, the tolerances should be eased as far as possible subject to the premise that the standard deviation of the kinematic motion deviation of the end-effector, which depend on the design variables t_i, are less than allowable values. Then, giving the allowance of the standard deviation of the kinematic motion deviation of the end-effector and taking each tolerance values as the constraints factors, the tolerance design of each component is converted into a constrained optimization problem, as shown in Eq. (20) - (21), which assumed that seven kinds of tolerances $t_i (i = 1\sim7)$ shown in Table 2 are design variables and that tolerance manufacturing cost is the objective function. The position of guide-ways $a\sim e$ in Fig.2 are indicated in Fig.6,7. Eq.(20) represents the relationship between dimensions and tolerances and formulated based on ISO Tolerance.

$$\min \ g = \sum_{i=1}^{7} \frac{r_i^{0.34}}{t_i} \quad (20)$$

Where, r_i is the dimension of the components.

$$f \le f_{max}, \ f = \sqrt{\sigma_x^2 + \sigma_y^2 + \sigma_z^2} \quad (21)$$

Table. 2 Design variables for seven kinds of tolerances

Symbol	Meaning	Guide-way
t_1	Radial axis	a
t_2	Radial bearing	b
t_3	Thrust bearing	c
t_4	Spherical joints (Ball)	d
t_5	Spherical joints (Socket)	e
t_6	Dimensional tolerance of the 1st link	
t_7	Dimensional tolerance of the 2nd link	

Where, f_{max} is the allowable range of the standard deviation of the kinematic deviation of the end-effector, and σ_i is standard deviations in i-direction of the position X_E.

6. Case Study

The proposed method is applied to the tolerance design of the parallel link robot shown in Fig. 3 by setting the allowable kinematic deviation to 0.05 mm. Fig. 8 shows the optimum solutions.

The designed tolerances of t_1, t_2 are smaller than other tolerance values, as shown in Fig. 8. This means that the kinematic motion deviations of end-effector is deeply influenced by tolerance values of those guide-ways, therefore those tolerance values are rather important to reduce the standard deviations of kinematic motion of the end-effector.

7. Conclusion

Systematic procedure is proposed to design both the geometric tolerances of the guide-ways connecting components and dimensional tolerances of the links, based on allowance of the kinematic motion deviations of the end-effector. This method is to design tolerances under the constraints on the kinematic motion deviations of the end-effector by applying mathematical models.

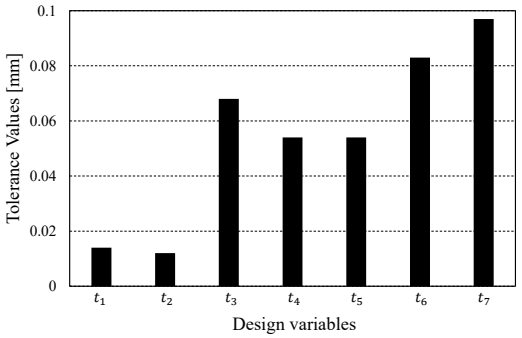

Fig. 8 The result of tolerance design values

8. References

[1] Carrino, L., Moroni, G., Polini, W. and Semeraro, W. (2001). 3D Tolerance analysis involving geometric tolerances, paper presented in *the 34th CIRP International Seminar of Manufacturing Systems*, Athens, Greece, pp. 29-38.

[2] Mathieu, L., Clement, A. and Bourdet, P. (1997). Modelling, representation, processing and inspection of tolerances: A survey, paper presented in *the 5th CIRP Seminar on Computer Aided Tolerancing*, Toronto, Canada, pp. 1-38.

[3] Narahari, Y., Sudarson, R., Lyous, K., Duffy, M. R. and Sriran, R. D. (1999). Design for tolerance of electro-mechanical assemblies: An integrated approach, *IEEE Transactions on Robotics and Automation*, vol. 15(6), pp. 1062-1079.

[4] Ngoi, B. K. A. and Agarwal, M. (1998). The generic capsule approach to tolerance stack analysis, *International Journal of Production Research*, vol. 36(12), pp. 3273-3293.

[5] Ngoi, B. K. A., Lim, B. H. and Ang, P. S. (2000). Nexus method for stack analysis of geometric dimensioning and tolerancing (GDT) problems, *International Journal of Production Research*, vol. 38(1), pp. 21-37.

[6] Roy, U., Liu, C. R. and Woo T. C. (1991). A review of dimensioning and tolerancing: Representation and processing, *Computer-Aided Design*, vol.23(7), pp. 466-483.

[7] Satonaka, N., Sugimura, N., Tanimizu, Y. and Iwamura, K. (2005). A study on modeling and analysis of kinematic motion deviations of machine tools (1st Report, Modeling and analysis of geometric deviations of constituting units), *Transactions of the JSME, Series C*, vol.71(708), pp. 192-198 (in Japanese).

[8] Satonaka, N., Sugimura, N., Tanimizu, Y. and Iwamura, K. (2007). Analysis of geometric deviations of machine products under Maximum Material Conditions, *Transactions of the JSME, Series C*, vol. 73(730), pp. 285-291(in Japanese).

[9] Satonaka, N., Sugimura, N., Tanimizu, Y. and Iwamura, K. (2008). A study on modeling and analysis of kinematic motion deviations of machine tools (2nd Report, Modeling and Analysis of Linear Tables and Machine Tools), *Transactions of the JSME, Series C*, Vol.74(737), pp. 198-205 (in Japanese).

[10] Sugimura, N., Watabiki, H., Thasana, W., Iwamura, K. and Tanimizu, Y. (2012). Analysis of Kinematic Motion Deviations of Rotary Tables Based on Geometric Tolerances, *Journal of Advanced Mechanical Design, Systems, and Manufacturing, JSME*, vol. 6(7), pp. 1132-1142.

[11] Takahashi, A., Yoshida, A., Thasana, W., Sugimura, N., Iwamura, K. and Tanimizu, Y. (2014). Analysis of Kinematic Motion Deviations of Machining Centers Based on Geometric Tolerances, *Journal of Advanced Mechanical Design, Systems, and Manufacturing, JSME*, vol. 8(4), pp. 1-12.

[12] Takematsu, R., Sugimura, N., Yoshida, A., Thasana, W., Tanimizu, Y. and Iwamura, K. (2015). A Study on Tolerance Design for Machine Tools based on Shape Generation Functions, paper presented in The 6th TSME International Conference on Mechanical Engineering (the 6th TSME-ICoME 2015), Hua-Hin, Thailand.

[13] Tsumura, T. and Ohnishi, K. (2001). Machine Design and Drawing Handbook based on JIS, Rikogakusya Co. Ltd. pp. 17-85 (in Japanese).